Age-related changes in mineralocorticoid receptors in rat hearts

DANLI HU[1,2], RUOLAN DONG[3], YANJUN ZHANG[4], YAN YANG[2], ZHIHUI CHEN[2],
YING TANG[2], MENGLU FU[2], XIZHEN XU[5,6] and LING TU[2]

[1]National Clinical Research Center of Cardiovascular Diseases, State Key Laboratory of Cardiovascular Disease,
Fuwai Hospital, National Center for Cardiovascular Diseases, Chinese Academy of Medical Sciences and
Peking Union Medical College, Beijing 100037; [2]Department of Geriatric Medicine; [3]Institute of Integrated
Traditional Chinese and Western Medicine, Tongji Hospital, Tongji Medical College, Huazhong University of
Science and Technology, Wuhan, Hubei 430030; [4]Department of Internal Medicine, Division of Cardiology,
General Hospital of Puyang Oil Field, Puyang, Henan 457001; [5]Department of Internal Medicine, Division of Cardiology,
Tongji Hospital, Tongji Medical College, Huazhong University of Science and Technology; [6]Hubei Key Laboratory
of Genetics and Molecular Mechanisms of Cardiological Disorders, Wuhan, Hubei 430030, P.R. China

Abstract. Age-related alterations in the renin-angiotensin-aldosterone system (RAAS) have been reported in the cardiovascular system; however, the detailed mechanism of the RAAS component mineralocorticoid receptors (MR) has not been elucidated. The present study aimed to investigate the associations between MR and cardiac aging in rats, as well as the regulatory effects of oxidative stress and mitochondrial abnormalities in the aging process. MR expression in the hearts of male Sprague-Dawley rats aged 3 months (young rats) and 24 months (old rats) was evaluated *in vivo*. In addition, *in vitro*, H9C2 cells were treated with a specific MR antagonist, eplerenone, in order to investigate the molecular mechanism underlying the inhibition of myocyte aging process. The results demonstrated that MR expression was significantly higher in 24-month-old rat hearts compared with in 3-month-old rat hearts. These changes were accompanied by increased p53 expression, decreased peroxisome proliferator-activated receptor γ coactivator-1α expression, decreased mitochondrial renewal as assessed by electron microscopy, increased oxidative stress and decreased superoxide dismutase. *In vitro*, selective antagonism of MR partially blocked H_2O_2-induced myocardial aging as assessed by p16, p21 and p53 expression levels and excessive reactive oxygen species (ROS) accumulation. These results indicated that increased MR expression may drive age-related cardiac dysfunction via mitochondrial damage, increased ROS accumulation and an imbalanced redox state.

Correspondence to: Dr Ling Tu, Department of Geriatric Medicine, Tongji Hospital, Tongji Medical College, Huazhong University of Science and Technology, 1095 Jiefang Avenue, Wuhan, Hubei 430030, P.R. China
E-mail: lingtu@tjh.tjmu.edu.cn

Dr Xizhen Xu, Department of Internal Medicine, Division of Cardiology, Tongji Hospital, Tongji Medical College, Huazhong University of Science and Technology, 1095 Jiefang Avenue, Wuhan, Hubei 430030, P.R. China
E-mail: xzxu@tjh.tjmu.edu.cn

Introduction

According to a 2017 United Nations report on the aging of the world population (1), the number of people aged ≥60 years worldwide will more than double by 2050, reaching ~2.1 billion (2-4). Aging is an independent risk factor for the incidence and prevalence of cardiovascular diseases, such as hypertension and atherosclerosis, which can lead to heart failure (5). Changes in the aging heart are mainly associated with structural and functional abnormalities of the cardiac muscle cells, including increased left ventricular wall thickness, cardiac fibrosis and impaired diastolic function (6,7). However, the molecular mechanisms underlying the decline in cardiac function during aging remain unknown.

Renin-angiotensin system (RAAS) activation is closely associated with the aging process and the etiology of cardiac diseases. Mineralocorticoid receptors (MR) are an important component of RAAS. The activated MR signal induced by a high salt load leads to fibrosis and cardiac dysfunction, independent of renal effects and elevated blood pressure (3). MR antagonists decrease morbidity and mortality in patients with heart failure; however, hyperkalemia, gynecomastia and erectile dysfunction limit their widespread use (8). In addition, cardiomyocyte-specific MR inactivation improves infarct healing, and prevents progressive adverse cardiac remodeling and contractile dysfunction (9). Identifying the cardiac-specific features of MR signaling may provide a basis for improving

cardiovascular conditions without compromising renal function.

Local myocardial RAAS activation is involved in age-associated cardiac remodeling. However, to the best of our knowledge, the dynamic expression of MR during the aging process has not been characterized. The aim of the present study was to investigate changes in MR expression in the aging heart, and to identify the relationship between these changes and oxidative stress and mitochondrial abnormalities.

Materials and methods

Experimental reagents. Rabbit primary polyclonal MR antibody (cat. no. 21854-1-AP) was obtained from ProteinTech Group, Inc. Mouse monoclonal antibodies against GAPDH (cat. no. sc-59540), p53 (cat. no. sc-71819), p16 (cat. no. sc-377412), p21 (cat. no. sc-817), peroxisome proliferator-activated receptor γ coactivator-1α (PGC-1α; cat. no. sc-518025), transforming growth factor-β1 (TGF-β1; cat. no. sc-130348), gp91-phox (cat. no. sc-130543), p47-phox (cat. no. sc-17845), p67-phox (cat. no. sc-374510), superoxide dismutase (SOD)-1 (cat. no. sc-101523) and SOD-2 (cat. no. sc-133134) were obtained from Santa Cruz Biotechnology, Inc. A horseradish peroxidase-conjugated goat anti-rabbit secondary antibody (cat. no. BA1056) and goat anti-mouse antibody (cat. no. BA1075) were obtained from Wuhan Boster Biological Technology, Ltd. Eplerenone (cat. no. HY-B0251) was purchased from MedChemExpress. All other chemicals and reagents were purchased from Sigma-Aldrich (Merck KGaA), unless otherwise specified.

Animals. All animals were fed normal chow and housed at 22°C and ~40-70% humidity under a 12-h light/dark cycle with free access to adequate food and water. Animal health and behavior were monitored once a week. All experimental procedures were approved by the Animal Research Ethics Board at Huazhong University of Science and Technology, and conformed to the Update of the Guide for the Care and Use of Laboratory Animals published by the National Research Council (US) Committee. All animal studies also complied with the ARRIVE guidelines (10) and the AVMA euthanasia guidelines (11).

In total, 16 male Sprague-Dawley rats (Hubei Provincial Animal Research Center, Hubei Provincial Center for Disease Control and Prevention) were divided into two groups (n=8 in each group): Young (age, 3 months; weight, 250-350 g) and old (age, 24 months; weight, 650-750 g). At the designated age of 3 or 24 months, rats were intraperitoneally anesthetized with 3% pentobarbital sodium (35-40 mg/kg body weight; Nembutal; Sumitomo Dainippon Pharma Co., Ltd.) and were then euthanized by cervical dislocation following the collection of blood samples. Animals suffering chronic diseases, such as tumors, respiratory failure and heart failure, as characterized by weight loss, a change in vital signs such as heart rate, breathing or hypothermia, and abnormal behavior, were immediately euthanized by cervical dislocation following anesthesia with 3% pentobarbital sodium (~35-40 mg/kg body weight) to relieve or end suffering in advance. The intestinal tumor of the rat (age, 18 months; weight, 550 g) in the old group weighed 6.2 g and the maximum tumor burden was ~1% (tumor weight/body weight). This animal displayed reduced consumption of food and water, and a subcutaneous mass in the abdomen. Cachexia index was ~2.9% of body weight, calculated according to the equation: [(Initial body weight-final body mass + mass of the tumor + control weight gain)/(initial body mass + mass gain control group)] x100 (12,13). Rats in the old group (age, 18 months old) showing signs of distress were sacrificed and their tissues were not used for subsequent experiments. Subsequently their hearts were excised, washed with saline, cleaned and weighed. Large vessels and connective tissues were removed, and the left ventricular cardiac tissues were stored at -80°C until subsequent experiments.

Reverse transcription-quantitative PCR (RT-qPCR). Total RNA was extracted from the left ventricle using TRIzol® reagent (cat. no. 15596026; Invitrogen; Thermo Fisher Scientific, Inc.) according to the manufacturer's protocol. First-strand cDNA was synthesized with 1 μg RNA using a cDNA Synthesis kit (cat. no. K1622; Thermo Fisher Scientific, Inc.) as previously described (14). The primers were designed using Primer 5.0 (Premier Biosoft International) and confirmed by BLAST (blast.ncbi.nlm.nih.gov/Blast.cgi) searches against the GenBank database (www.ncbi.nlm.nih.gov/genbank). The sequences of primers were as follows: *Nr3c2*, forward 5'-AGTGGGGTCCATCGGCAG-3', reverse 5'-CCTCTGTCTTAGGGAAAGGAACG-3'; and β-actin, forward 5'-AGTGTGACGTTGACATCCGT-3' and reverse 5'-GACTCATCGTACTCCTGCTT-3'. A SYBR Green-based master mix (cat no. A25742; Thermo Fisher Scientific, Inc.) was used to amplify the cDNA using an ABI Prism 7700 sequence detection system (Thermo Fisher Scientific, Inc.). Thermocycling conditions were as follows: 40 cycles of 95°C for 15 sec and 60°C for 1 min. The results were analyzed using the $2^{-\Delta\Delta Cq}$ method (14).

Western blot analysis. The heart tissue homogenate was centrifuged at 14,000 x g for 15 min at 4°C and resolved in RIPA lysis buffer (Beyotime Institute of Biotechnology) containing a protease inhibitor cocktail. Protein concentration was determined using the bicinchoninic acid assay kit (Beyotime Biotechnology, Wuhan). Loading volume of each sample was calculated in order to load 80 μg protein per lane. After protein quantification, appropriate amount of 6x sample loading buffer was added, and samples were boiled at 95°C for 5 min. The suspension was separated by 10% SDS-PAGE and transferred onto a PVDF membrane. The membranes were blocked using 5% BSA for 1.5 h at room temperature. The membranes were incubated overnight at 4°C with primary antibodies against MR (ProteinTech Group, Inc.), and p16, p21, p53, PGC-1α, SOD-1, TGF-β1, gp91-phox, p47-phox, p67-phox and SOD-2 (Santa Cruz Biotechnology, Inc.), at a final dilution of 1:1,000. The membranes were then incubated for 2 h at room temperature (27°C) with a horseradish peroxidase-conjugated secondary antibody (cat. no. BA1056; Wuhan Boster Biological Technology, Ltd.), diluted to 1:10,000. Following exposure using a Luminescent Imaging system (Tanon Science and Technology Co., Ltd.), blots were washed and re-incubated with monoclonal GAPDH antibody as a control. Protein expression levels were normalized to the

corresponding GAPDH levels, as determined using Gel-Pro Analyzer 4 (Media Cybernetics, Inc.).

Hemodynamic measurements and echocardiography. Body weight was recorded during the experiments. Blood pressure measurements were obtained at room temperature using a photoelectric tail-cuff system (PowerLab; ADInstruments). The cardiac function of rats was analyzed using a VIVO 2100 echocardiography machine (VisualSonics, Inc.); for analysis of cardiac function, sedation of the rats was induced with 4% inhaled isoflurane (cat. no. R510-22; RWD Life Science Co., Ltd.) and anesthesia was subsequently maintained with 2% isoflurane for ~8 min (0.2-0.3 l/min). The rats exhibited a steady heart rate (350-400 beats/min) and breathing, as previously described (15).

Wheat germ agglutinin (WGA) fluorescence staining. Fresh-frozen heart sections (8 μm) were washed with phosphate-buffered saline three times and incubated with FITC-conjugated WGA (Beyotime Institute of Biotechnology) diluted to 50 μg/ml for 1 h in the dark. After washing out the dye, images were obtained using a fluorescence microscope (magnification, x200). All steps were performed in the dark.

Electron microscopy. Following previously published protocols (16), fresh left ventricle specimens were fixed in 2.5% glutaraldehyde for 2 h, post-fixed in 1% osmium tetroxide for 2 h at 4˚C, dehydrated, embedded in epoxy resin at 30˚C for 4 h and sectioned (30-40 nm). Finally, the sections were double stained with 0.5% uranyl acetate and 1% lead citrate for 10 min at room temperature. A morphometric analysis was performed to determine mitochondrial damage using a Tecnai G 12 transmission electron microscope (FEI; Thermo Fisher Scientific, Inc.), as previously described (17).

Picrosirius red staining. Heart fibrosis was evaluated by Picrosirius Red staining. Fresh left ventricular heart tissues were fixed with 4% paraformaldehyde for 24 h at room temperature, were dehydrated by an increasing alcohol series and treated with xylene for 1 h at room temperature. Specimens were embedded in paraffin at 57˚C and cut into 4-5-μm-thick sections. Paraffin-embedded left ventricle sections (4-5 μm) were dewaxed and stained using a Picrosirius Red Staining kit (Nanjing Jiancheng Bioengineering Institute) according to the manufacturer's protocol. Images were obtained using a Nikon inverted light microscope (Nikon Corporation).

Dihydroethidium (DHE) histological staining. Fresh-frozen heart specimens were incubated with DHE diluted to 1:1,000 (cat. no. S0063; Beyotime Institute of Biotechnology), as previously described (18). Images were obtained using a fluorescence microscope (magnification, x200).

Immunohistochemical staining. Fresh left ventricular heart tissues were fixed with 4% paraformaldehyde for 24 h at room temperature, dehydrated by an increasing alcohol series, and treated with xylen for 1 h. Specimens were embedded with paraffin at 57˚C and cut into 4-5-μ-thick sections. Endogenous peroxidase activity was inhibited by 0.3% H_2O_2 solution for 10 min at room temperature and samples were blocked using 5% BSA for 20 min both at room temperature. Sections were incubated with an appropriate MR antibody (1:100 dilution; cat. no. 21854-1-AP; ProteinTech Group, Inc.) at 4˚C overnight. Following application of the biotinylated secondary antibody at a dilution of 1:100 at room temperature for 1 h (cat. no. BA1003; Wuhan Boster Biological Technology, Ltd.), samples were developed with DAB substrates. Images were captured using a Nikon light inverted microscope (Nikon Corporation) and analyzed using Image-Pro Plus 6 (Media Cybernetics, Inc.).

H9C2 cell culture and treatment. H9C2 rat cardiomyocytes (American Type Culture Collection) were cultured in DMEM supplemented with 10% BSA (Gibco; Thermo Fisher Scientific, Inc.), 100 IE/ml penicillin and 100 μg/ml streptomycin at 37˚C in an atmosphere of 5% CO_2/95% air. At 70-80% confluence, H9C2 cells were starved with 5% BSA for 6 h and then pre-treated with eplerenone (1 μM; cat. no. HY-B0251) at 37˚C 1 h before H_2O_2 (200 μM) was added for 2 h at 37˚C. The cells were then harvested for subsequent experimentation.

Statistical analysis. SPSS (version 19.0; IBM Corp.) was used to analyze data. All data are presented as the means ± standard error of the mean. Data from *in vivo* experiments conforming to the normal distribution and homogeneity of variances were analyzed by two-sample t-tests. One way ANOVA was used to evaluate differences among the four *in vitro* groups and the LSD t-test was used for pairwise comparisons between the groups. $P<0.05$ was considered to indicate a statistically significant difference.

Results

Effects of aging on cardiac morphology and hemodynamics. The tumor suppressor p53, an aging marker, and TGF-β, a marker of extracellular matrix synthesis and degradation, were examined in rat hearts by western blot analysis (19,20). As expected, age-related increases in the expression levels of p53 and TGF-β were observed (Fig. 1A-C). Hemodynamic results indicated that the systolic blood pressure of old rats was much higher than that of young rats, whereas the difference in diastolic blood pressure between the two groups was not significant (Fig. 1D). This indicated that the isolated systolic hypertension of older rats was similar to that of humans (21). To clarify the development of the aging heart, morphological characteristics were examined. WGA staining demonstrated that the area of cardiomyocytes was much greater in the old group compared with in the young group (Fig. 1E and F). Cardiac fibrosis in aging rats was evaluated by Picrosirius Red staining. As shown in Fig. 1G and H, collagen accumulation in the myocardial interstitial and perivascular regions was markedly increased in the 24-month-old group compared with in the 3-month-old group.

Aging-related alterations in cardiac function. Echocardiography indicated that there was a significant age-associated decrease in ejection fraction (Fig. 2A) and fractional shortening (FS) (Fig. 2B) in the old rats compared with in the young animals. Conversely, the heart weight/body weight ratio was greater in the rats aged 24 months compared with in
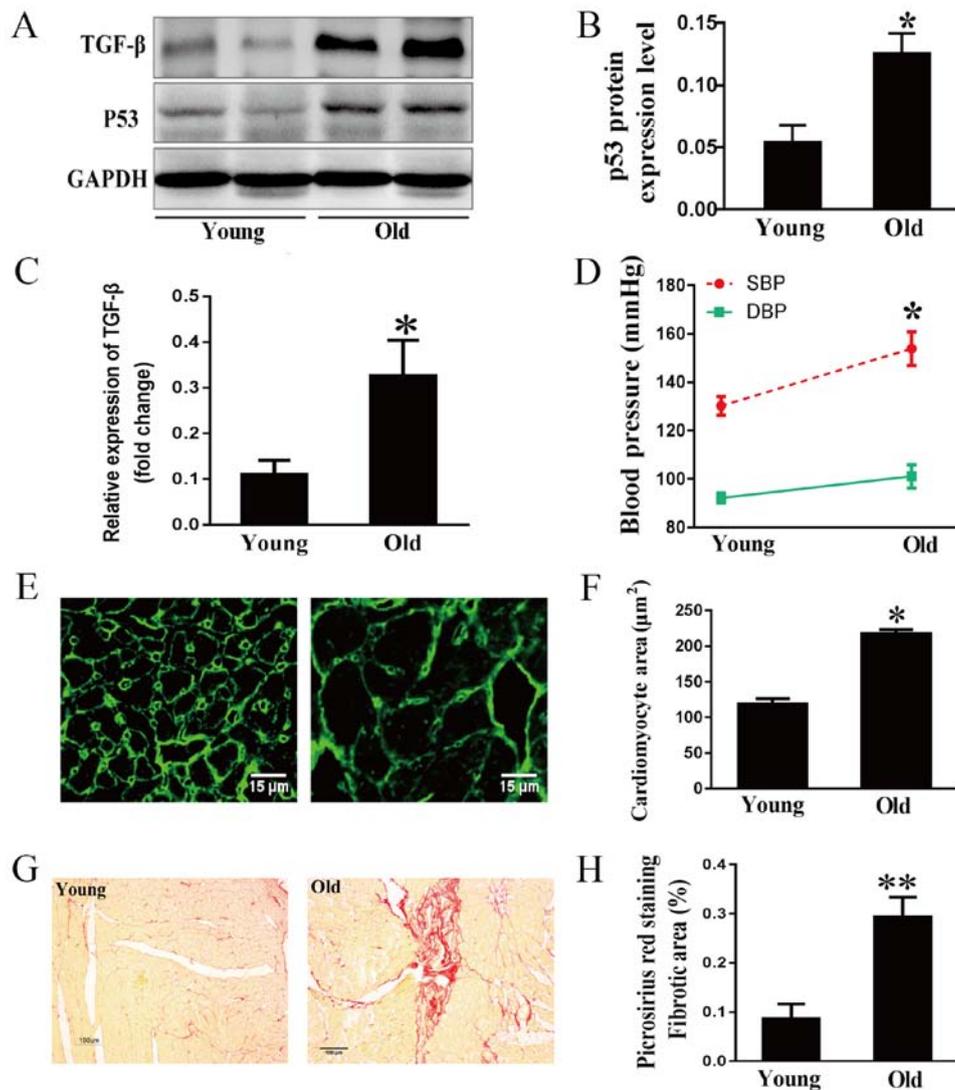
Figure 1. Effects of aging on myocardial hypertrophy and fibrosis. (A) Representative immunoblots, and (B) semi-quantification for p53 and (C) TGF-β1 in cardiac tissues. (D) SBP and DBP of 3- and 24-month-old rats. (E) Cardiomyocyte area determined by WGA staining and (F) the corresponding semi-quantification of WGA staining; scale bar, 15 μm. (G) Myocardial interstitial and perivascular fibrosis stained by Picrosirius red and (H) the corresponding semi-quantification; scale bar, 100 μm. Data are presented as the means ± standard error of the mean from each group; n=8 per group. $^*P<0.05$, $^{**}P<0.01$ vs. young group. DBP, diastolic blood pressure; SBP, systolic blood pressure; TGF-β1, transforming growth factor-β1.

the rats aged 3 months (Fig. 2C). As shown in Fig. 2D and E, the interventricular septum at end-diastole (IVS-d) and the left interventricular posterior wall at end-diastole (LVPW-d) were thicker in 24-month-old rats compared with in 3-month-old rats. These data indicated that aging may impair cardiac diastolic function.

Increased MR expression in the aging heart. Activation of the renin-angiotensin-aldosterone system (RAAS) is considered an important cause of hypertension and cardiac diseases in the aging population (22). However, the mechanism underlying RAAS activation at the onset and development of cardiomyopathy during the aging process remains to be elucidated. Therefore, MR mRNA expression was examined. As shown in Fig. 3A, the mRNA expression of MR was two-fold higher in the older group compared with in the younger group. Additionally, MR protein expression in the older hearts was approximately double that in the younger hearts (Fig. 3B and C). As determined by immunohistochemical analysis, the average optical

density of MR in the older hearts was more than double that in the younger hearts (Fig. 3D and E).

Effects of aging on mitochondrial structure and cardiac function. It has previously been reported that the aging process is closely related to obvious alterations in mitochondrial structure (23). In this study, cardiac ultrastructure was examined by electron microscopy. As shown in Fig. 4A, myocardial mitochondria were enlarged, swollen and lacked cristae in 24-month-old rats. PGC-1α drives all aspects of mitochondrial biogenesis and cardiac function, including mitochondrial number, mitochondrial respiration and ROS levels (24-27). Mitochondrial dysfunction induces a profound p53-dependent decrease in PGC-1α, resulting in impaired oxidative phosphorylation and ATP generation (25). As expected, PGC-1α expression was lower in the older group compared with in the younger group (Fig. 4B and C). These data suggested that aging may aggravate the impaired mitochondrial ultrastructure and function.
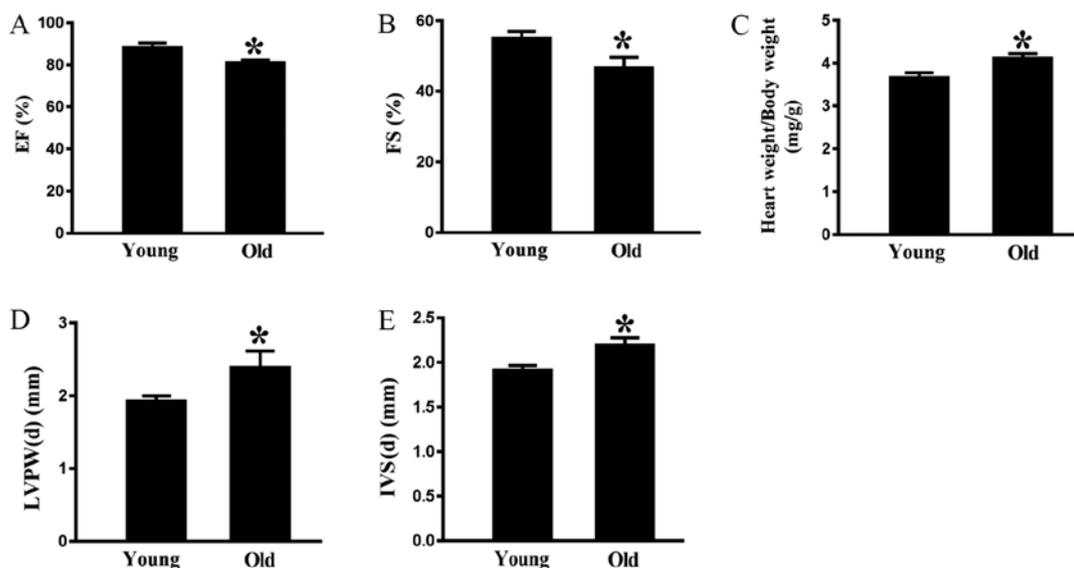
Figure 2. Effects of aging on cardiac function. (A) EF and (B) FS were measured by echocardiography. (C) Ratio of heart weight to body weight was detected after the rats were sacrificed. (D) LVPW-d and (E) IVS-d were determined by echocardiography. Data are presented as the means ± standard error of the mean from each group; n=8 per group. *P<0.05 vs. young group. EF, ejection fraction; FS, fractional shortening; IVS-d, interventricular septal thickness at end-diastole; LVPW-d, left ventricular posterior wall thickness at end-diastole.
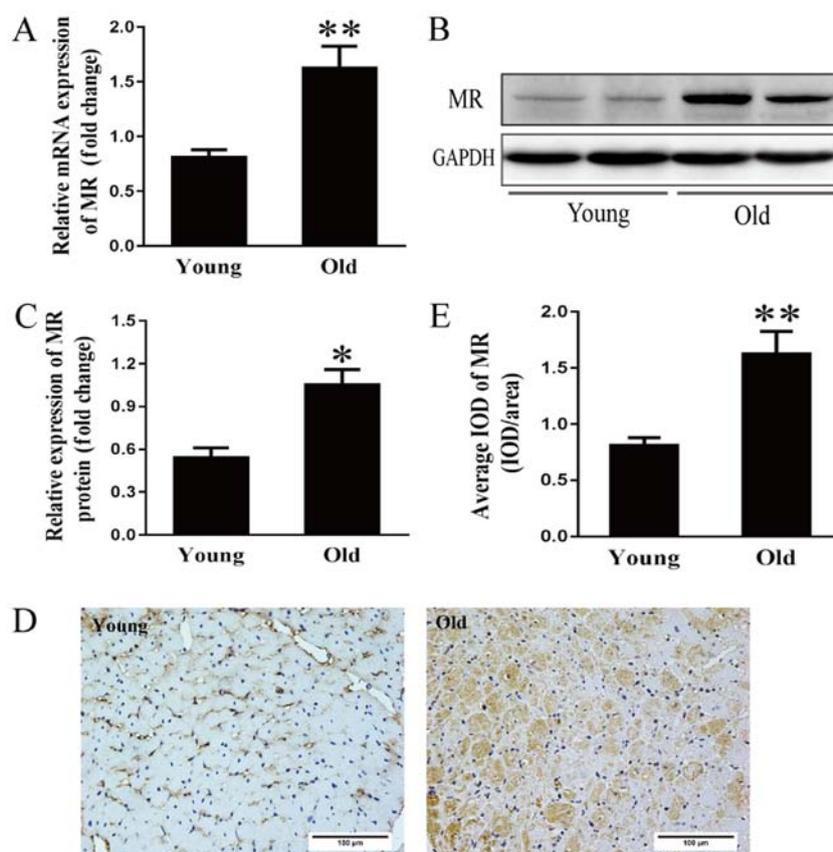
Figure 3. Increased MR expression in the aging heart. (A) Reverse transcription-quantitative PCR analysis of MR mRNA expression in 3- and 24-month-old rats. (B) Representative immunoblots and (C) semi-quantification of MR in the hearts of the two groups. (D) Immunohistochemical staining and (E) corresponding semi-quantification of MR expression in the hearts of young (3 months) and old (24 months) rats; scale bar, 100 μm. Data are presented as the means ± standard error of the mean from each group; n=8 per group. *P<0.05, **P<0.01 vs. young group. IOD, integrated optical density; MR, mineralocorticoid receptors.

Effects of aging on oxidative stress and the redox state. DHE fluorescence staining was performed to examine ROS production in the aging hearts. As shown in Fig. 4D and E, DHE fluorescence intensity was stronger in 24-month-old rats
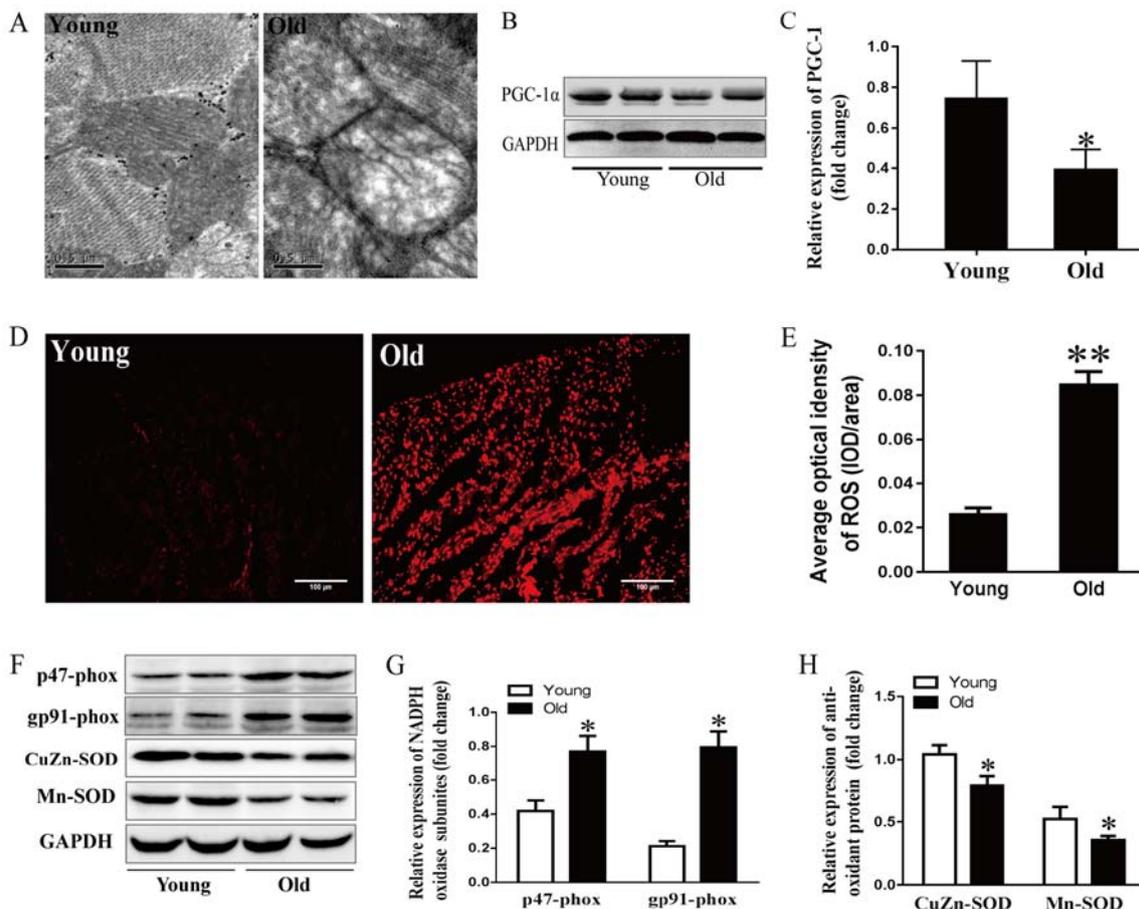
Figure 4. Effects of aging on mitochondrial stress and the redox state. (A) Mitochondrial ultrastructure of myocytes detected by electron microscopy; scale bar, 0.5 μm. (B) Representative immunoblots and (C) semi-quantitation of PGC-1α. (D) ROS levels detected by DHE fluorescence staining and (E) corresponding semi-quantification; scale bar, 50 μm. (F) Representative immunoblots of p47-phox, gp91-phox, CuZn- and Mn-SOD. (G) Semi-quantification of p47-phox and gp91-phox. (H) Semi-quantification of CuZn-SOD and Mn-SOD. Data are presented as the means ± standard error of the mean from each group; n=8 per group. *P<0.05, **P<0.01 vs. young group. DHE, dihydroethidium; NADPH, nicotinamide adenine dinucleotide phosphate; PGC-1α, peroxisome proliferator-activated receptor γ coactivator-1α; ROS, reactive oxygen species; SOD, superoxide dismutase.

compared with in the younger rats, indicating that more ROS was generated and accumulated in the aging left ventricular myocytes. The tissue levels of ROS are regulated by ROS generation and antioxidant enzymes. The present study detected subunits of nicotinamide adenine dinucleotide phosphate (NADPH) oxidase, including p47-phox and gp91-phox, and the antioxidant enzyme SOD. As shown in Fig. 4F-H, p47-phox and gp91-phox levels were higher in the 24-month-old group compared with the younger group, whereas SOD-1- and SOD-2-levels were lower in the older group.

MR antagonism suppresses H$_2$O$_2$-induced cardiac aging and mitochondrial dysfunction in vitro. To establish the relationship between MR and cardiac mitochondrial abnormalities, H9C2 cells were treated with H$_2$O$_2$ to mimic cardiomyocyte aging. H$_2$O$_2$ treatment increased the expression of the aging markers p16 and p21 (Fig. 5A). Additionally, H$_2$O$_2$ administration decreased the expression of p53-dependent PGC-1α and stimulated excess production of ROS (Fig. 5). Eplerenone, an MR antagonist, effectively blocked these effects, illustrating that MR blockage partially alleviated aging-induced mitochondrial abnormalities. Furthermore, cardiomyocytes induced by H$_2$O$_2$ demonstrated higher expression levels of

NADPH oxidase subunits and lower antioxidant contents, suggesting that aging exacerbated the imbalanced redox state. Eplerenone treatment markedly reversed the upregulation of p47-phox, p67-phox and gp91-phox, and increased the levels of SOD-1 and SOD-2. These data suggested that MR antagonism partially protected against aging via mitochondria dysfunction and oxidative stress.

Discussion

The results of the present study indicated that the hearts of aging rats exhibited altered RAAS components, characterized by enhanced MR expression. The altered expression of MR was accompanied by cardiac dysfunction, increased fibrosis, mitochondrial damage and an imbalanced redox state in aging hearts.

Cardiac aging manifests as increased left ventricular thickness, enlarged chamber size, increased fibrosis and diastolic dysfunction (7,28,29). In the present study, aging induced cardiac remodeling, including myocyte hypertrophy, interstitial fibrosis and subsequent diastolic dysfunction, as characterized by decreased FS and increased IVS-d and LVPW-d. These data suggested that the aging rat model was
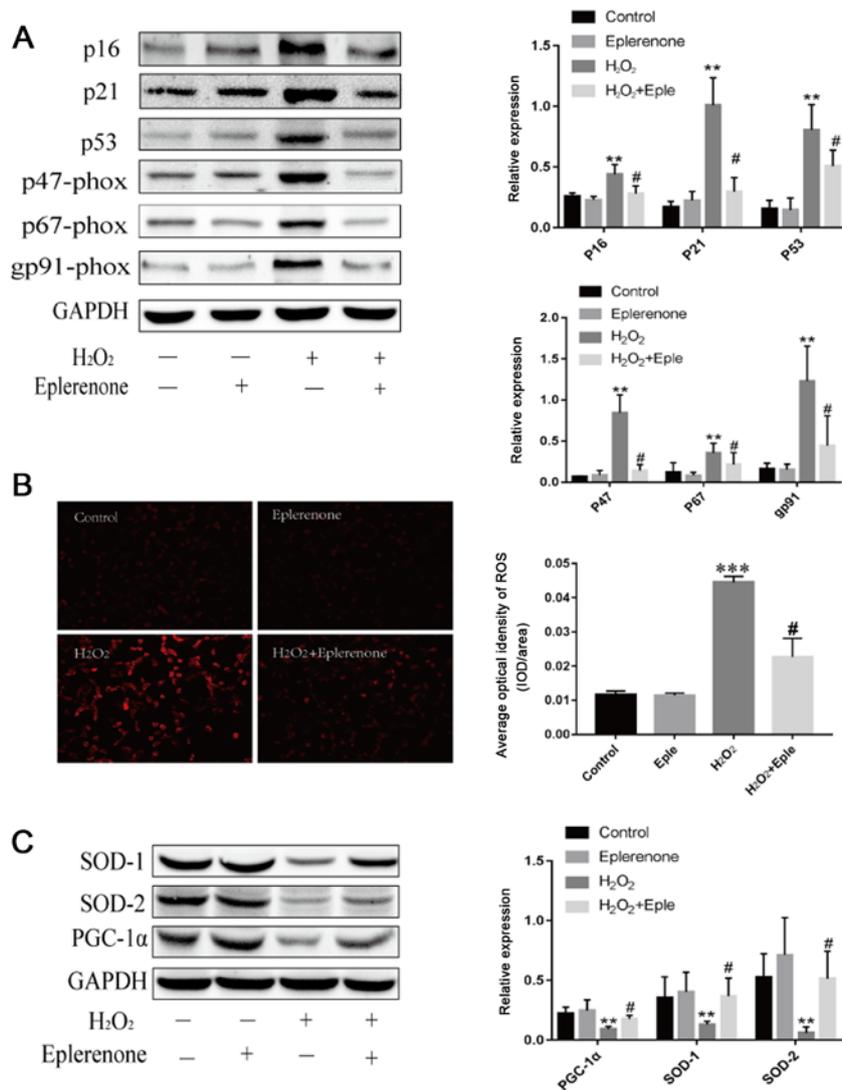
Figure 5. MR antagonism suppresses H_2O_2-induced cardiac aging and mitochondrial dysfunction. (A) Immunoblotting and semi-quantification of p16, p21, p53 and NADP subunits, p47-phox, p67-phox and gp91-phox expression in H9C2 cells. Protein expression levels were normalized to GAPDH. (B) ROS levels detected by DHE staining in H9C2 cells following different treatments (magnification, x100; scale bar, 100 μm). (C) SOD-1, SOD-2 and PGC-1α protein expression levels detected by western blotting. Data are representative of three experiments, n=3. **P<0.01 and ***P<0.001 vs. control group; #P<0.05 vs. H_2O_2 group. DHE, dihydroethidium; MR, mineralocorticoid receptors; PGC-1α, peroxisome proliferator-activated receptor γ coactivator-1α; ROS, reactive oxygen species; SOD, superoxide dismutase; Eple, eplerenone.

sufficient to investigate the potential mechanisms underlying the role of MR in age-related cardiac dysfunction.

The activation of local RAAS components has been demonstrated in various tissues. Intrarenal RAAS activation is associated with the renal aging process (30,31). Enhanced vascular RAAS activation is associated with arterial aging (32) and age-related cardiac remodeling involves myocyte RAAS activation (33). MR signaling is a terminal effector in RAAS, and exerts more cardiac actions than aldosterone, due to the absence of 11β hydroxysteroid dehydrogenase type 2 (HSD2) in the heart, making cortisol (or corticosterone in rodents) the predominant ligand for MR (34). Previous research has indicated that the conditional cardiac-specific overexpression of human MR in mice generates a high rate of arrhythmia-related sudden death (35). Cardiomyocyte-specific MR deficiency improves infarct healing, and prevents progressive adverse cardiac remodeling (9) and deoxycorticosterone/salt-induced tissue inflammation and remodeling

by blocking the recruitment of macrophages to the myocardium (3). Loss of cardiomyocytes-derived MR protects the transaortic constriction model from cardiac dilatation and failure; however, MR knockout does not prevent the development of cardiac remodeling and an inflammatory response after pressure overload (4). In the present study, the protein and mRNA expression levels of MR in the aging model of fibrosis were approximately two-fold higher than those in younger rats, indicating that the increased expression of MR in myocytes of aging hearts may exacerbate cardiac remodeling and cardiac dysfunction. MR expression in adult rat hearts (12-month-old) rose moderately (data not shown), suggesting that cardiomyocyte MR may serve a universal role during the whole aging process. However, whether MR accumulation in hearts is elevated in healthy older humans and its potential clinical implications remain to be investigated.

The p53 tumor suppressor, a cellular stress sensor, is an aging marker, as evidenced by the early aging phenotypes of

p53-mutant mice (19). PGC-1α is a master regulator of mitochondrial biogenesis and renewal, and interacts with p53 by post-transcriptional regulation (24,36). Aging is characterized by reduced renewal of mitochondria and an impaired ultrastructure (37,38), and this is mainly ascribed to decreased PGC-1α activity. The p53-induced PGC-1α mitochondrial/metabolic axis integrates many factors involved in the aging process in the heart (25). The present study indicated that 24-month-old rats exhibited damaged mitochondrial architecture and reduced PGC-1α. It also indicated that the increased MR level in aging hearts may be associated with impaired mitochondrial structure and decreased mitochondrial biogenesis renewal via p53-induced PGC-1α downregulation.

Cellular ROS sources are mainly composed of mitochondrial and extramitochondrial sources, e.g., membrane NADPH oxidase. The mitochondrial respiratory chain, particularly complex I and complex III, is the major cellular source of ROS (39). NADPH oxidases are multi-protein enzyme complexes that generate superoxide by the catalysis of electron transfer from NADPH to molecular oxygen (40). Myocytes are rich in mitochondria, in order to accommodate their high demand for ATP, and mitochondria are the major targets of free radicals (41,42). Therefore, mitochondria are vulnerable to ROS and are particularly susceptible to oxidative stress damage (43). In the present study, mitochondrial damage and increased cellular ROS accumulation were observed. These changes may be associated with alterations in MR expression.

The tissue ROS balance is precisely regulated by the ROS generation system and antioxidant enzyme system. NADPH oxidase catalyzes electron passage to molecular oxygen, whereas SOD converts superoxide into H_2O_2 and then catalyzes H_2O_2 into H_2O and O_2, in sequence (44). In the present study, the aging heart exhibited increased p47-phox and gp91-phox expression from NADPH oxidase, and reduced SOD expression. These data suggested that the age-associated MR increase may be accompanied by increased ROS generation and decreased antioxidant enzymes in the aging heart.

Further *in vitro* analyses demonstrated that cardiomyocyte aging induced by H_2O_2 markedly upregulated the expression of the aging markers p16 and p21, and induced an imbalanced redox state. In addition, an imbalanced redox state, including increased p47-phox, p67-phox and gp91-phox expression, and reduced SOD1 and SOD2 expression, further increased ROS accumulation. Eplerenone partially antagonized aging-induced cardiomyocyte damage and improved the imbalanced redox state. These results suggested that these protective effects were partly mediated by MR activation.

The increase in MR activation may be a key pathogenic factor that links aging-related mitochondrial dysfunction to cardiac aging in rats. In addition, the results of the present study indicated that the increase in age-associated MR expression may lead to mitochondrial dysfunction, increased oxidative stress and cardiac remodeling via an imbalance in the p53/PGC-1α axis. Further studies are required to clarify the interaction between MR and age-related mitochondrial dysfunction, and to clarify whether the antagonism of MR in hearts can delay the progression of cardiac aging and prolong lifespan.

In conclusion, the results of the present study suggested that an increase in MR may serve an important role in age-related cardiac dysfunction by decreasing mitochondrial renewal mediated by the p53/PGC-1α metabolic axis, impairing mitochondrial ultrastructure and inducing accumulation of ROS. Further investigation of MR in the pathophysiology of cardiac aging may facilitate the understanding of the mechanism underlying the protective effects of MR antagonists in aging-induced cardiac dysfunction, and it may be a suitable therapeutic target for delaying age-related cardiac dysfunction and increasing longevity.

Availability of data and materials

The datasets used and/or analyzed during the current study are available from the corresponding author on reasonable request.

Authors' contributions

DH designed the experiments, performed the research and wrote the manuscript. RD and YY analyzed data. YZ, ZC, YT and MF performed the experiments. LT conceived and designed the study, and gave final approval of the version to be published. XX analyzed and interpreted the data, and revised the manuscript. All authors read and approved the final manuscript.

Ethics approval and consent to participate

All animal experiments were approved by the Animal Research Ethics Board at Huazhong University of Science and Technology and conformed to the Guide for the Care and Use of Laboratory Animals published by the National Institutes of Health. The present study was approved by the ethics committee of Tongji Hospital.

Patient consent for publication

Not applicable.

Competing interests

The authors declare that they have no competing interests.

References

1. United Nations, Department of Economic and Social Affairs, Population Division: World Population Ageing 2017 - Highlights (ST/ESA/SER.A/397). United Nations, New York, NY, 2017. https://www.un.org/en/development/desa/population/publications/pdf/ageing/WPA2017_Highlights.pdf.
2. Wyss-Coray T: Ageing, neurodegeneration and brain rejuvenation. Nature 539: 180-186, 2016.

3. Rickard AJ, Morgan J, Bienvenu LA, Fletcher EK, Cranston GA, Shen JZ, Reichelt ME, Delbridge LM and Young MJ: Cardiomyocyte mineralocorticoid receptors are essential for deoxycorticosterone/salt-mediated inflammation and cardiac fibrosis. Hypertension 60: 1443-1450, 2012.

4. Lother A, Berger S, Gilsbach R, Rösner S, Ecke A, Barreto F, Bauersachs J, Schütz G and Hein L: Ablation of mineralocorticoid receptors in myocytes but not in fibroblasts preserves cardiac function. Hypertension 57: 746-754, 2011.

5. López-Otin C, Blasco MA, Partridge L, Serrano M and Kroemer G: The hallmarks of aging. Cell 153: 1194-1217, 2013.

6. Biernacka A and Frangogiannis NG: Aging and cardiac fibrosis. Aging Dis 2: 158-173, 2011.

7. Boyle AJ, Shih H, Hwang J, Ye J, Lee B, Zhang Y, Kwon D, Jun K, Zheng D, Sievers R, et al: Cardiomyopathy of aging in the mammalian heart is characterized by myocardial hypertrophy, fibrosis and a predisposition towards cardiomyocyte apoptosis and autophagy. Exp Gerontol 46: 549-559, 2011.

8. Pitt B, Zannad F, Remme WJ, Cody R, Castaigne A, Perez A, Palensky J and Wittes J: The effect of spironolactone on morbidity and mortality in patients with severe heart failure. randomized aldactone evaluation study investigators. N Engl J Med 341: 709-717, 1999.

9. Fraccarollo D, Berger S, Galuppo P, Kneitz S, Hein L, Schütz G, Frantz S, Ertl G and Bauersachs J: Deletion of cardiomyocyte mineralocorticoid receptor ameliorates adverse remodeling after myocardial infarction. Circulation 123: 400-408, 2011.

10. Kilkenny C, Browne W, Cuthill IC, Emerson M and Altman DG; NC3Rs Reporting Guidelines Working Group: Animal research: Reporting in vivo experiments: The ARRIVE guidelines. Br J Pharmacol 160: 1577-1579, 2010.

11. AVMA Guidelines for the Euthanasia of Animals: 2013 Edition. American Veterinary Medical Association, Schaumburg, IL, 2013. https://www.avma.org/KB/Policies/Documents/euthanasia.pdf?fb-clid=IwAR3ffStVgfUcSvHHKHbzCIE0VoVh8riNyIJ2HpqAJVxGF3NjaPc4-2AKO5Q

12. Padilha CS, Borges FH, Costa Mendes da Silva LE, Frajacomo FTT, Jordao AA, Duarte JA, Cecchini R, Guarnier FA and Deminice R: Resistance exercise attenuates skeletal muscle oxidative stress, systemic pro-inflammatory state, and cachexia in Walker-256 tumor-bearing rats. Appl Physiol Nutr Metab 42: 916-923, 2017.

13. Guarnier FA, Cecchini AL, Suzukawa AA, Maragno AL, Simão AN, Gomes MD and Cecchini R: Time course of skeletal muscle loss and oxidative stress in rats with Walker 256 solid tumor. Muscle Nerve 42: 950-958, 2010.

14. Livak KJ and Schmittgen TD: Analysis of relative gene expression data using real-time quantitative PCR and the 2(-Delta Delta C(T)) method. Methods 25: 402-408, 2001.

15. Lai J, Chen F, Chen J, Ruan G, He M, Chen C, Tang J and Wang D: Overexpression of decorin promoted angiogenesis in diabetic cardiomyopathy via IGF1R-AKT-VEGF signaling. Sci Rep 7: 44473, 2017.

16. Mascorro JA and Bozzola JJ: Processing biological tissues for ultrastructural study. Methods Mol Biol 369: 19-34, 2007.

17. Feng W, Xu X, Zhao G, Zhao J, Dong R, Ma B, Zhang Y, Long G, Wang DW and Tu L: Increased Age-related cardiac dysfunction in bradykinin B2 receptor-deficient mice. J Gerontol A Biol Sci Med Sci 71: 178-187, 2016.

18. Takimoto E, Champion HC, Li M, Ren S, Rodriguez ER, Tavazzi B, Lazzarino G, Paolocci N, Gabrielson KL, Wang Y and Kass DA: Oxidant stress from nitric oxide synthase-3 uncoupling stimulates cardiac pathologic remodeling from chronic pressure load. J Clin Invest 115: 1221-1231, 2005.

19. Tyner SD, Venkatachalam S, Choi J, Jones S, Ghebranious N, Igelmann H, Lu X, Soron G, Cooper B, Brayton C, et al: p53 mutant mice that display early ageing-associated phenotypes. Nature 415: 45-53, 2002.

20. Chen T, Li J, Liu J, Li N, Wang S, Liu H, Zeng M, Zhang Y and Bu P: Activation of SIRT3 by resveratrol ameliorates cardiac fibrosis and improves cardiac function via the TGF-β/Smad3 pathway. Am J Physiol Heart Circ Physiol 308: H424-H434, 2015.

21. Susic D, Varagic J and Frohlich ED: Isolated systolic hypertension in elderly WKY is reversed with L-arginine and ACE inhibition. Hypertension 38: 1422-1426, 2001.

22. Neves MF, Cunha AR, Cunha MR, Gismondi RA and Oigman W: The role of renin-angiotensin-aldosterone system and its new components in arterial stiffness and vascular aging. High Blood Press Cardiovasc Prev 25: 137-145, 2018.

23. Cheng Z, Ito S, Nishio N, Thanasegaran S, Fang H and Isobe K: Characteristics of cardiac aging in C57BL/6 mice. Exp Gerontol 48: 341-348, 2013.

24. Sahin E, Colla S, Liesa M, Moslehi J, Müller FL, Guo M, Cooper M, Kotton D, Fabian AJ, Walkey C, et al: Telomere dysfunction induces metabolic and mitochondrial compromise. Nature 470: 359-365, 2011.

25. Moslehi J, DePinho RA and Sahin E: Telomeres and mitochondria in the aging heart. Circ Res 110: 1226-1237, 2012.

26. Leone TC and Kelly DP: Transcriptional control of cardiac fuel metabolism and mitochondrial function. Cold Spring Harb Symp Quant Bio76: 175-182, 2011.

27. Lehman JJ, Barger PM, Kovacs A, Saffitz JE, Medeiros DM and Kelly DP: Peroxisome proliferator-activated receptor gamma coactivator-1 promotes cardiac mitochondrial biogenesis. J Clin Invest 106: 847-856, 2000.

28. Bonda TA, Szynaka B, Sokolowska M, Dziemidowicz M, Winnicka MM, Chyczewski L and Kamiński KA: Remodeling of the intercalated disc related to aging in the mouse heart. J Cardiol 68: 261-268, 2016.

29. Burks TN, Marx R, Powell L, Rucker J, Bedja D, Heacock E, Smith BJ, Foster DB, Kass D, O'Rourke B, et al: Combined effects of aging and inflammation on renin-angiotensin system mediate mitochondrial dysfunction and phenotypic changes in cardiomyopathies. Oncotarget 6: 11979-11993, 2015.

30. Yoon HE and Choi BS: The renin-angiotensin system and aging in the kidney. Korean J Intern Med 29: 291-295, 2014.

31. Uneda K, Wakui H, Maeda A, Azushima K, Kobayashi R, Haku S, Ohki K, Haruhara K, Kinguchi S, Matsuda M, et al: Angiotensin II Type 1 receptor-associated protein regulates kidney aging and lifespan independent of angiotensin. J Am Heart Assoc 6: pii: e006120, 2017.

32. Yoon HE, Kim EN, Kim MY, Lim JH, Jang IA, Ban TH, Shin SJ, Park CW, Chang YS and Choi BS: Age-associated changes in the vascular renin-angiotensin system in mice. Oxid Med Cell Longev 2016: 6731093, 2016.

33. Wang M, Zhang J, Walker SJ, Dworakowski R, Lakatta EG and Shah AM: Involvement of NADPH oxidase in age-associated cardiac remodeling. J Mol Cell Cardiol 48: 765-772, 2010.

34. Young MJ and Rickard AJ: Mineralocorticoid receptors in the heart: Lessons from cell-selective transgenic animals. J Endocrinol 224: R1-R13, 2015.

35. Ouvrard-Pascaud A, Sainte-Marie Y, Bénitah JP, Perrier R, Soukaseum C, Nguyen Dinh Cat A, Royer A, Le Quang K, Charpentier F, Demolombe S, et al: Conditional mineralocorticoid receptor expression in the heart leads to life-threatening arrhythmias. Circulation 111: 3025-3033, 2005.

36. Sen N, Satija YK and Das S: PGC-1α, a key modulator of p53, promotes cell survival upon metabolic stress. Mol Cell 44: 621-634, 2011.

37. Viña J, Gomez-Cabrera MC, Borras C, Froio T, Sanchis-Gomar F, Martinez-Bello VE and Pallardo FV: Mitochondrial biogenesis in exercise and in ageing. Adv Drug Deliv Rev 61: 1369-1374, 2009.

38. López-Lluch G, Irusta PM, Navas P and de Cabo R: Mitochondrial biogenesis and healthy aging. Exp Gerontol 43: 813-819, 2008.

39. Sahin E and Depinho RA: Linking functional decline of telomeres, mitochondria and stem cells during ageing. Nature 464: 520-528, 2010.

40. Bedard K and Krause KH: The NOX family of ROS-generating NADPH oxidases: Physiology and pathophysiology. Physiol Rev 87: 245-313, 2007.

41. Tsutsui H, Kinugawa S and Matsushima S: Mitochondrial oxidative stress and dysfunction in myocardial remodelling. Cardiovasc Res 81: 449-456, 2009.

42. Di Lisa F, Kaludercic N, Carpi A, Menabó R and Giorgio M: Mitochondria and vascular pathology. Pharmacol Rep 61: 123-130, 2009.

43. Gomez-Cabrera MC, Sanchis-Gomar F, Garcia-Valles R, Pareja-Galeano H, Gambini J, Borras C and Viña J: Mitochondria as sources and targets of damage in cellular aging. Clin Chem Lab Med 50: 1287-1295, 2012.

44. Rajamohan SB, Raghuraman G, Prabhakar NR and Kumar GK: NADPH oxidase-derived H(2)O(2) contributes to angiotensin II-induced aldosterone synthesis in human and rat adrenal cortical cells. Antioxid Redox Signal 17: 445-459, 2012.